

MODELING THE PERFORMANCE OF THE LSST IN SURVEYING THE NEAR-EARTH OBJECT POPULATION

T. GRAV

Planetary Science Institute, Tucson, AZ 85719, USA; tgrav@psi.edu

A. K. MAINZER

Jet Propulsion Laboratory, California Institute of Technology, Pasadena, CA 91109, USA

T. SPAHR

NEO Sciences, LLC

(Dated:)

ABSTRACT

We have performed a detailed survey simulation of the LSST performance with regards to near-Earth objects (NEOs) using the project’s current baseline cadence. The survey shows that if the project is able to reliably generate linked sets of positions and times (a so-called “tracklet”) using two detections of a given object per night and can link these tracklets into a track with a minimum of 3 tracklets covering more than a ~ 12 day length-of-arc, they would be able to discover 62% of the potentially hazardous asteroids (PHAs) larger than 140 m in its projected 10 year survey lifetime. This completeness would be reduced to 58% if the project is unable to implement a pipeline using the two detection cadence and has to adopt the four detection cadence more commonly used by existing NEO surveys. When including the estimated performance from the current operating surveys, assuming these would continue running until the start of LSST and perhaps beyond, the completeness fraction for PHAs larger than 140 m would be 73% for the baseline cadence and 71% for the four detection cadence. This result is a lower completeness than the estimate of [Ivezić et al. \(2007\)](#) and [Ivezić et al. \(2014\)](#); however the result is quite close to that of [Jones et al. \(2016\)](#) who show completeness $\sim 70\%$ using the identical survey cadence as used here. We show that the traditional method of using absolute magnitude $H < 22$ mag as a proxy for the population with diameters larger than 140m results in completeness values that are too high by $\sim 5\%$. Our simulation makes use of the most recent models of the physical and orbital properties of the NEO and PHA populations, as well as simulated cadences and telescope performance estimates provided by the LSST project. The consistency of the results presented here when compared to those of [Jones et al. \(2016\)](#) demonstrates the robustness of these survey modeling approaches. We also show that while neither LSST nor a space-based IR platform like NEOCam individually can complete the survey for 140m diameter NEOs, the combination of these systems can achieve that goal after a decade of observation.

Keywords: asteroids, surveys

1. INTRODUCTION

As Earth travels through space along its orbit around the Sun it traverses through a population of asteroids and comets, termed the near-Earth objects (NEOs; asteroids and comets that approach within 1.3 au of the Sun). With regularity, Earth finds itself on a collisional course with one of these NEOs. Most of the time the objects are small and burn up in the atmosphere, but sometimes the NEO is large enough that it can cause

damage. The effects can range from the local damage caused by the Tunguska airburst in 1908 ([Chyba et al. 1993](#)) or the Chelyabinsk airburst in 2013 ([Brown et al. 2013](#); [Kohout et al. 2014](#)), to the regional destruction caused by the impact that created the kilometer-sized Meteor Crater in Arizona ([Grieve 1987](#)). There is even evidence that the effects can be global, as seen in the theory that an impactor in the Cretaceous-Paleogene era caused the enormous ring-shaped feature beneath

the Gulf of Mexico and significantly contributed to the extinction of the dinosaurs (Alvarez *et al.* 1980).

Over the last few decades, Congress has tasked NASA with two goals to address the NEO detection problem, in part spurred by the impact of Comet Shoemaker-Levy 9 into Jupiter (Hammel *et al.* 1995; Zahnle & Mac Low 1994). The first goal, also called the Spaceguard survey, concerned the population of objects larger than 1km in diameter and directed the agency to detect 90% of this population by 2008. Mainzer *et al.* (2011a) showed that this goal was reached somewhere in 2010. The second goal was given in the George E. Brown, Jr. near-Earth object section of the NASA Authorization Act of 2005 (Public Law 109-155), which charged the agency to discover and track 90% of the NEO population with diameters larger than 140m by 2020.

The current NEO survey capability is dominated by the Catalina Sky Survey (CSS; Larson 2007) and the Pan-STARRS project (Denneau *et al.* 2013). Both surveys operate in similar fashion by observing each pointing on the sky 4-5 times per night, with each return to the same pointing being separated by minutes to tens of minutes. Detections in the fields are connected into tracklets, and when their motions are consistent with that of the NEO population they are posted as candidate NEOs on the Minor Planet Center (MPC) NEO confirmation page. In many cases other observers, dubbed the follow-up community, provide further observations over the next few nights that refine the orbit and establish whether or not the candidate was indeed an NEO. Originally the Pan-STARRS project planned to adopt a two detections per night (hereafter 2-detection) survey cadence for its wide-field multi-science survey. Due to a variety of problems, the Pan-STARRS project was forced to change its survey cadence to the more traditional four detections per night (hereafter 4-detection) cadence that has proven to be successful in CSS, NEOWISE (Mainzer *et al.* 2011b), and now Pan-STARRS. See Denneau *et al.* (2013) for a description of the Pan-STARRS Moving Object Processing System (MOPS), including the details of its performance and its problems. New cameras, such as the Dark Energy Camera (DECam; Diehl & Dark Energy Survey Collaboration 2012), together with refined false detection handling through for example machine learning algorithms Goldstein *et al.* (see 2015) may yet provide the advances to solve this problem in the future (although at present these techniques are not yet widely implemented for NEO surveys).

The known NEO population currently consists of more than 13,800 objects, $\sim 1,500$ of which were discovered in 2015 (<http://neo.jpl.nasa.gov/stats/>). The Catalina Sky Survey has been leading the NEO survey effort during most of the last decade, but when Pan-STARRS went from a multi-science survey telescope to a dedi-

cated NEO survey telescope in early 2014, its discovery rate increased by 60%. This elevated Pan-STARRS to the premier discovery telescope in 2015, responsible for 48.6% of the discoveries for that year. CSS was the second largest discoverer in 2015, responsible for 36.2% of the discoveries. However, some caution must be exercised when considering where the increase in discoveries took place. The increase in the yearly discovery rate from 2011 to 2015 has been 74.2%, with 1,563 discoveries in 2015 compared to 897 in 2011. However, the increase in the yearly discovery rate of the larger objects (absolute magnitude $H < 22$ mag, traditionally considered to be objects larger than 140m in diameter) is only 34.5% over the same time period, with 526 discovered in 2015 compared to 391 in 2011. The fraction of objects discovered per year that have $H > 22$ mag has steadily increased from 56.4% in 2011 to 67.6% in 2015. This trend continues into the first two months on 2016.

In 2003 NASA commissioned a report that concluded that a number of ground-based, space-based, and networked systems are capable of meeting the goal set forth in the George E. Brown, Jr. goal (Stokes *et al.* 2003). The National Research Council released a report in 2010 that came to a similar conclusion (Shapiro *et al.* 2010). Several projects have been proposed to address this problem, but detailed simulations of most of these proposals have not been published in the refereed literature. We performed a detailed study of an infrared space-based option in Mainzer *et al.* (2015), where we compared the completeness for NEO population with diameters larger than 140m for a Venus-trailing orbit and a L1 halo orbit. Sentinel, a privately funded infrared space-based survey, proposed by the B612 Foundation (Lu *et al.* 2013), is similar to the Venus-trailing orbit studied in Mainzer *et al.* (2015). The L1 halo orbit option, named the Near-Earth Object Camera (NEOCam), has been submitted to the 2005, 2010, and 2014 NASA Discovery Announcements. NEOCam has received funding in 2010 to continue the development of its infrared detector technology (McMurtry *et al.* 2013) and was selected for Phase 2 development in the 2014 Discovery Announcement Opportunity. Mainzer *et al.* (2015) concluded that the L1 halo option offered superior performance to the Venus-trailing option when considering integral survey completeness for NEOs larger than 140m in diameter, even when the effects of the loss of data rate in a Venus-trailing orbit is neglected.

In this paper we examine a complementary ground based option, the Large Synoptic Survey Telescope (LSST; Ivezić *et al.* 2007; Ivezić *et al.* 2014), an 8.4m telescope (with the approximate effective collective area of a 6.67m in diameter mirror) with a 9.6 square degree imager that is currently being built in Chile with funding

from the National Science Foundation and the Department of Energy. We perform detailed survey simulations using the latest population models based on NEOWISE results (Mainzer et al. 2011a, 2012a) and the most current model of the survey plan provided by LSST project and compare our results with others published by the LSST project (Ivezić et al. 2007; Ivezić et al. 2014). These results are compared to the best available results from the space-based L1 halo orbit survey option. We also show that assuming that using absolute magnitude $H < 22$ mag as a proxy for the population with diameters larger than 140m is not a valid approximation.

1.1. The LSST Project

The effectiveness all surveys for NEO discovery depends on the details of their performance and observational cadence. As the baseline LSST survey cadence is currently envisioned, each pointing will be visited two time per night. This will produce a 6 band (u , g , r , i , z , and y filters) wide-field deep astronomical survey covering more than 20,000 square degrees of southern sky, visiting each pointing on the sky over 1000 times in a 10 year survey.

In Ivezić et al. (2007), the LSST team presented a simulation that used a set of 1000 synthetic orbital elements that match the distribution of discovered objects in the large size range where present surveys were essentially complete. The simulation computed the positions of the synthetic orbits every 5 days and used a filtering method based on the assumed sky coverage and cadence pattern, limiting magnitude of the survey, visibility constraints, and observing conditions. They estimated that the LSST baseline cadence can achieve, over 10 years, a completeness of 90% for PHAs larger than 250m in diameter, and 75% completeness for those with diameters larger than 140m. They further suggested that ongoing simulations showed that improvements in filter choices and operations, LSST would be capable of reaching a completeness of 90% for PHAs larger than 140m in ten years, but details of these optimizations were not discussed. In Ivezić et al. (2014) a size-limited complete sample of 800 known PHAs was used as the trial population. This simulation improved upon the previous simulation by determining which PHAs are present in each exposure and whether they were bright enough to be detected in individual exposures. They found that the baseline cadence provides orbits for 82% of the PHAs larger than 140m in diameter after 10 years of operations. It was suggested that optimization of certain aspects of the survey operations would improve the completeness to 90% in 12 years without significantly affecting the survey’s other science goals. It is important here to note that sizes quoted in these papers are derived by converting absolute magnitudes using an aver-

age albedo. We will show in our results why this is not an optimal approach, resulting in completeness values that are overly optimistic.

2. THE SIMULATIONS

In the last few years our knowledge of the NEO population has increased significantly. Mainzer et al. (2011a, 2012a) used the asteroid-detection portion of the Wide-field Infrared Survey Explorer’s (WISE; Wright et al. 2010) data processing pipeline (NEOWISE; Mainzer et al. 2011b) to update the estimate of the number of objects larger than 140m in diameter and to derive new size and albedo distributions for the NEO population as a whole, as well as the subpopulations. This has allowed us to create a new synthetic NEO population that is based on both the known NEO orbital population (Grav et al. 2011) and these new distributions of sizes and albedos (see Section 2.3 for the details). Significant work has also been done by the LSST project, resulting in the production of an improved baseline cadence that features the latest knowledge of the telescope and instrument performance, weather and seeing conditions at the Cerro Pachón site, and improvements based on earlier cadence simulations. With these recent developments, we present a set of survey simulations that combine our updated NEO population model with the most recent cadence and performance simulations provided by the LSST project to investigate the performance of the LSST project in surveying the NEO population.

2.1. 2 versus 4 Detections per Night

One of the major features of the LSST baseline cadence is the use of the 2-detection approach, which deviates from the way the current NEO surveys operate. CSS, PanSTARRS and NEOWISE all require 4-5 detections per night to reliably link detections of individual object due to the large range of rates and directions of most NEOs. This number of repeated observations per night has been shown to be relatively robust against the noise points, image artifacts, cosmic rays, and other transient sources that degrade the reliability of position-time pairs (so-called “tracklets”) constructed from fewer detections per night (Denneau et al. 2013; Mainzer et al. 2011b; Cutri et al. 2012).

Since the baseline assumes a 2-detection cadence that has not yet been tested and validated for NEO discovery, the LSST project has also produced a 4-detection cadence, which is more similar to the cadences used by the current NEO surveys. These two cadences are described in more detail in Section 2.4.

In Mainzer et al. (2015), we assumed that 4 detections spaced over 8-9 hours were required to reliably link detections of an individual object to form a tracklet. Requiring additional detections dramatically increases

tracklet reliability but decreases the rate at which fresh sky can be covered, so the performance of 2-detection surveys cannot be compared with those of 4-detection surveys. Should a 2-detection cadence be proven a viable means of linking tracklets through future testing and validation, space-based surveys can also adopt this approach. Therefore, to compare the relative performance of the LSST survey and the L1 halo-orbit infrared space-based survey in discovering and tracking NEOs, we have elected to simulate both the 2- and 4-detection cadences. This work provides the bounding cases for the expected performance of these two options and allows accurate comparisons to be made.

2.2. The Solar System Survey Simulator

The solar system survey simulator we have created to analyze the performance of LSST is essentially the same as that used to model the performance of a 0.5m thermal infrared space telescope in Mainzer *et al.* (2015). The technique begins by combining a frame-by-frame pointing list for the simulated survey with a population of synthetic moving objects whose positions and velocities are computed at the epoch of each frame. The brightness and on-sky velocity of each object as it appears in each frame is evaluated to determine whether or not it would have been detected in that exposure, depending on that frame’s estimated sensitivity. If sets of detections are found in a cadence that allows them to be uniquely linked to one another over a sufficiently long timespan, the object can be declared “*discovered*”. The survey cadence is critically important in determining which objects merely pass through the field of regard, and which objects are actually detected, discovered, and tracked. This simulation does not yet include models of background sources or other image artifacts and transient sources (such as noise, cosmic rays, defective pixels, scattered light, etc.) that can confuse or break linkages; therefore, these simulations should be regarded as a best case.

If a set of two 4-detection tracklets covering an average of 10-20 nights or more can be linked to one another, an asteroid’s orbit can be determined with sufficient accuracy to allow it to not only be declared discovered, but to allow it to be recovered at its next apparition. A set of at least three 2-detection tracklets is needed to allow the same for the 2-detection cadence. The survey simulation in Mainzer *et al.* (2015) describes a method for tallying detections over a survey cadence that collects tracklets spanning ~ 10 -22 days. In this paper, we apply a similar technique to simulate the performance of the LSST project, adopting the baseline survey cadence given on the LSST Operations Simulation (Op-

Sim) website¹ (Connolly *et al.* 2014; Jones *et al.* 2014). This frame-by-frame simulation is combined with our synthetic population model to predict the numbers of objects that would be detected in each frame.

To give a robust estimate of the variation in orbital elements and physical properties, our simulations include 25 synthetic populations generated randomly according to the size distribution, albedo distribution, and numbers specified in Mainzer *et al.* (2012a). By running many populations through the survey simulator, we can evaluate systematic uncertainties introduced by the limits of our knowledge of the NEO population. The ephemeris for each synthetic object was computed at each frame time using the SWIFT numerical integrator (Levison & Duncan 1994), which implements the Bulirsch-Stoer integration method, on the high performance computing facilities at Jet Propulsion Laboratory. Objects were assumed to be successfully assembled into tracklets if they were detected two or more times per night, with an on-sky velocity between 0.011 and 3.2°/day. The slow speed limit of $\sim 0.011^\circ/\text{hour}$ is set by the LSST average seeing of ~ 0.5 - 1 arcsec and the minimum estimated separation between two consecutive exposures in a night of ~ 30 minutes. The upper speed limit of is determined by the need to avoid significant trailing losses in a 15 sec exposure.

We note here that these velocity limits have virtually no effect on the completeness fraction of these survey simulations as we focus on the population larger than 140m. For these larger objects the distances at which they are observed are such that their velocities naturally fall within these limits. However, for objects smaller than 140m, the effects of trailing can have a significant impact on the completeness fraction as these objects have to be much closer to the observatory to be detectable and thus generally have much higher velocities with respect to the observer. For the baseline cadence, tracklets were considered successfully linked if three tracklets, each containing at least two detections each, were detected over the course of ~ 12 days. This requires that a single 2-detection tracklet can be successfully linked to another 2-detection tracklet no later than 6 days after, which as noted above has not been yet proven to be workable to date; we do not address this issue at present in our simulation. For the 4-detection cadence, an object was considered a discovery if two tracklets, each with at least four detections, are found within a 12 day timespan. This timespan was selected from our experience with the current surveys, where follow-up and linking has proven to be extremely difficult after

¹ <https://confluence.lsstcorp.org/display/SIM/Operations+Simulator+Benchmark+Surveys>

10-12 days, based on a 4-5 detection discovery tracklet (Cutri et al. 2012; Mainzer et al. 2011b; Denneau et al. 2013).

As noted in Mainzer et al. (2015), any survey simulation must account for the performance of the existing surveys such as the CSS and PanSTARRS, both in terms of the number of objects they have already discovered to date, and in terms of the number of objects they would be expected to discover over the course of the future survey. It should be noted that the LSST survey patterns available from the OpSim start in 1994 and run 10 years from this date. To estimate the overlap in discoveries between LSST and the historical and current surveys, it was therefore necessary to shift our historical and current survey simulations by 28 years back in time or shift the LSST cadence 28 years into the future (assuming that the LSST survey will start in 2022). This allowed us to derive a known population of NEOs that is similar to that which LSST will have when it starts its survey late this decade. Both methods yielded similar completeness fractions and similar overlap fractions with the existing surveys.

2.3. The Synthetic Near-Earth Object Population

The NEO population has historically been divided into several subpopulations. Starting from the outside and going inward, we consider four separate subpopulations in this paper: 1) the Amors, objects with perihelion distance in the range $1.017 < q \leq 1.3$ au; 2) the Apollos, which have orbits with semi-major axis $a \geq 1$ au and perihelion distance $q \leq 1.017$ au; 3) the Atens, which have orbits with semi-major axis $a < 1$ au and aphelion distance $Q \geq 0.983$ au; and 4) the interior Earth objects (IEOs), which have aphelion distances $Q < 0.983$ au. In addition, we use the term potentially hazardous asteroid (PHA) to indicate objects that are larger than 140m (the definition is usually given as absolute magnitude $H < 22$ mag rather than size) and have minimum-orbital-intersection-distance (MOID) less than 0.05 au (Ostro & Giorgini 2004).

Mainzer et al. (2011a) determined based on the results of the NEOWISE survey that there are $20,500 \pm 3,000$ near-Earth asteroids (NEAs; near-Earth comets were not included in the study) larger than 100 m in diameter. They looked at the subpopulations of the NEA population in Mainzer et al. (2012a) using the same data and determined that there are $1,600 \pm 760$ Atens larger than 100 m in diameter. The corresponding numbers for the Apollo and Amor subpopulations are $11,200 \pm 2,900$ and $7,700 \pm 3200$, respectively. This is similar to the results of Greenstreet et al. (2012), which is based on numerical simulations of dynamical evolution of objects from the main asteroid belt source regions into NEO space. Since NEOWISE does not provide an estimate of the IEOs, we

use the result of Greenstreet et al. (2012) as the basis to generate a population of interior objects that consist of 350 ± 100 objects (which is close to the 1.6% fraction given in their paper). The orbital elements for the Atens, Apollos, and Amors were generated based on the Grav et al. (2011) synthetic solar system model, which is in turn based on the Bottke et al. (2002) model.

In Mainzer et al. (2012a) each of the subpopulations was found to have a slightly different size and albedo distribution, and our synthetic populations reflect these differences. Since no measure of the size or albedo distribution of the IEOs exists, we use the distributions for the NEOWISE Aten population to generate sizes and albedos for the IEO population.

Since the LSST survey collects exposures in each of six bands, we need to model the magnitude of the synthetic NEOs at each wavelength. The absolute magnitude H was found for each object using the relation

$$H = -5 \cdot \log_{10} \left(\frac{D\sqrt{p_v}}{1329} \right), \quad (1)$$

where D is the assumed diameter in km and p_v is the assumed geometric visible albedo (Bowell et al. 1989). Each object's V band magnitude was computed using the IAU phase curve correction:

$$V(\alpha) = H + 5 \log(R\Delta) - 2.5 \log[(1-G)\Phi_1(\alpha) + G\Phi_2(\alpha)], \quad (2)$$

where R is the heliocentric distance in AU, Δ is the geocentric distance in AU, α is the Sun-observer-object angle, G is the magnitude-phase relationship slope parameter, and Φ_i are given in Bowell et al. (1989). The magnitude in the g band, H_g , is converted from the V band by $g = V + 0.56(B - V) - 0.12$, where $B - V = (g - r + 0.23)/1.05$ (Fukugita et al. 1996). Colors were generated in the *ugriz* system using the color distributions found in Ivezić et al. (2001), assigning C-type and S-type to each synthetic asteroid among the NEOs. While there are of course several other taxonomic classes found in the NEO population, the vast majority of objects are consistent with the two major classes (Binzel et al. 2002; Mainzer et al. 2011a).

2.4. LSST Survey Patterns

The two survey patterns used in this paper were generated by the LSST team and are available at their website. The most recent version of the baseline cadence is labeled *enigma_1189*. The baseline cadence executes 5 science proposals: 1) the Wide-Fast-Deep survey, which is the universal cadence that covers large fractions (about 75%) of the sky in pairs of exposures taken 15 to 60 minutes apart; 2) the Galactic Plane survey, which collects 30 visits in each of the 6 bandpasses; 3) the North Ecliptic survey, which covers the ecliptic in the universal cadence beyond the $+20^\circ$ declination limit set

in the Wide-Fast-Deep survey; 4) the South Pole survey, which like the Galactic plane survey collects 30 visits in each bandpass; and 6) 6 deep drilling fields for supernova surveying. The baseline cadence starts and stops observing at 12° twilight and uses the CTIO 4m weather log as its weather model. It uses the latest telescope model and includes scheduled downtime for maintenance; slews and filter changes together take 6.4 sec on average. The baseline cadence only uses the u filter approximately 6 days per lunation. The 4-detection cadence is labeled *enigma.1266*. This survey cadence follows the same design and criteria as the baseline, with the only significant difference being that each pointing is observed four times if possible.

The two LSST cadences are represented in Figures 1 to 4. The surveys cover solar elongations from opposition (at 180°) to about 60° , but only about 11% of the observations are at solar elongations lower than 90° for the baseline cadence (see Figure 1). This number drops to $\sim 7\%$ for the 4-detection cadence. Such limited coverage of these low-elongation regions will severely limit the usefulness of LSST in detecting objects in the IEO population, as these objects never rise above 90° solar elongation. The 5σ limiting magnitudes given by the published simulated survey cadences in each filter are very similar for the two cadences, with mean limiting magnitudes in each filter being 23.7, 24.7, 24.4, 23.7, 22.5 and 21.5 (for u , g , r , i , z and y , respectively). It should be noted that though the seeing distributions are similar for the two cadences, the airmass distributions are not. The 2-detection baseline cadence spends significantly more time at higher airmasses, which is most likely due to increased time spent at lower solar elongations and the fact that more sky is covered each night. Therefore, more of the observations are made at less favorable airmasses. We note here that these 5σ limiting magnitudes are similar to those given in Ivezic *et al.* (2014), but with lower values in the z and y filters, which we assume are due to the project having more recent values for the performance and observing conditions when these filters are used. The limiting magnitudes and solar elongation coverage presented here are at odds with Myhrvold (2016); his Figure 7 shows much fainter limiting magnitudes than presented here. While Myhrvold (2016) cites the possibility and capability of LSST observing at much smaller solar elongations, this is inconsistent with the published cadences provided by the LSST project and would potentially interfere with its other science goals. Additionally, Myhrvold (2016) incorrectly assumes that an object need only be detected once for it to be counted as discovered, cataloged, and tracked.

2.5. Detector Gaps

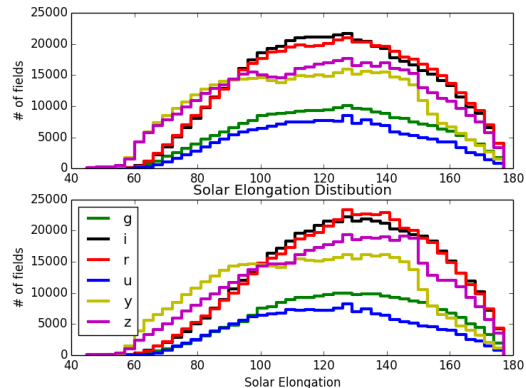


Figure 1. The solar elongation distribution of the LSST cadences in each filter. The baseline 2-detection cadence is given in the top panel, while the 4-detection cadence is shown in the lower panel.

LSST aims to have less than 5% of the focal plane lost due to gaps, bad pixels, or dead detectors. With a pixel size of 10 microns, which equals 0.2 arc seconds of sky for the LSST telescope, we assumed gaps that were 1 mm wide, or equivalent to 100 pixels. There are 21 “rafts” in the LSST focal plane design, with each raft containing a 3x3 array of 4k by 4k pixel CCDs. This yields 14 gaps in both the horizontal and vertical direction, for a total loss due to gaps that is close to 5% of the focal plane. Increasing the gaps between chips increases the probability of a detection being lost due to falling in a gap, particularly in the case of the 2-detection cadence, where loss of a single detection results in loss of the entire tracklet.

3. RESULTS

We first examine the population of NEOs with $H < 22$ mag, which has been the traditional way of reporting completeness in pursuit of the George E. Brown, Jr. goal. To do this, it was necessary to simulate a population of objects as small as diameters of 70m, since high albedo objects with that size would have $H \sim 22$ mag.

The results given in Ivezic *et al.* (2007) and Ivezic *et al.* (2014) are stated in terms of the completeness for

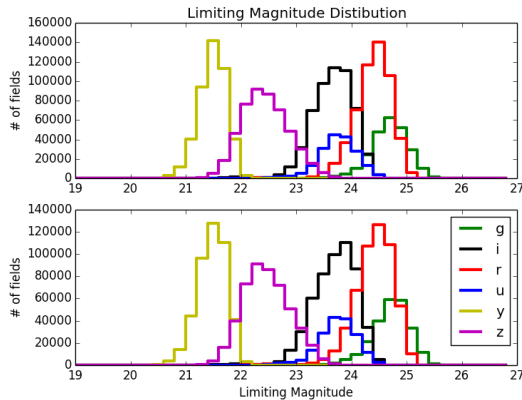


Figure 2. The 5σ limiting magnitude distribution of the LSST cadences in each filter. The baseline 2-detection cadence is given in the top panel, while the 4-detection cadence is shown in the lower panel.

the fraction of the population with absolute magnitudes brighter than $H = 22$ mag. If we consider the population with $H < 22$ mag, we achieve comparable numbers for this population in our simulations. In the 4-detection cadence, our simulations yield a survey completeness of 63% for the PHA population with $H < 22$ mag, increasing to 67% completeness for the same population in the 2-detection case. This is 8% lower than the 75% completeness reported in Ivezic et al. (2007) and 15% less than the 82% reported in Ivezic et al. (2014). The lower completeness in our simulations can be attributed to the higher fidelity simulations (field-by-field simulation, inclusion of gaps in the focal plane, actual accounting of individual detections needed to form tracklets and tracks), improved knowledge of the population model over the last decade, and better understanding of the performance of the telescope itself. An example of this is the visible magnitude distribution of the detections for the discovered objects in our simulations as seen in Figure 5. The distribution of V magnitudes turns over sharply at $V \sim 23.5 - 23.75$. This is inconsistent with Figure 7 in Myhrvold (2016), who assumes 50% limiting magnitudes ~ 0.8 mag fainter than our computations indicate.

However, examination of our improved population

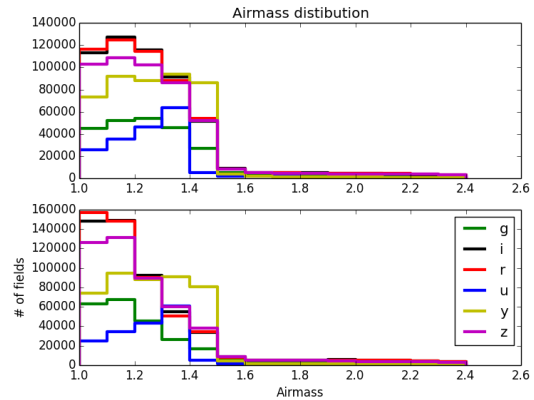


Figure 3. The airmass distribution of the LSST cadences in each filter. The baseline 2-detection cadence is given in the top panel, while the 4-detection cadence is shown in the lower panel.

models, which now use the size and albedo distributions directly based on the results from the NEOWISE survey (Mainzer et al. 2011a, 2012a), shows that $H < 22$ mag is a poor proxy for the NEO population with diameters larger than 140m. Approximately one quarter, 23%, of the NEOs with diameters larger than 140m have absolute magnitudes fainter than this due to the observed spread in NEO albedos (see Figure 6). Integrating over the albedo distribution of the NEO population the 90% integral completeness yields $H \sim 22.8$ for the 140m population. (E. Wright, personal communication). Setting the target as the population with $H < 22$ mag allows the surveys to discover a large number of high albedo objects with sizes as small as 70m, while a dark, large object with diameter of 370m and 2% albedo would be outside the population with $H = 22.02$ mag. This effect would be to increase the apparent effectiveness of visible-band surveys, as many objects with diameters less than 140m would erroneously be counted in the $H < 22$ mag tally. Thus, to correctly predict survey completeness, it is necessary to use synthetic populations that properly account for the actual size and albedo distributions of the NEOs, rather than simply assuming $H = 22$ mag corresponds to $D = 140$ m.

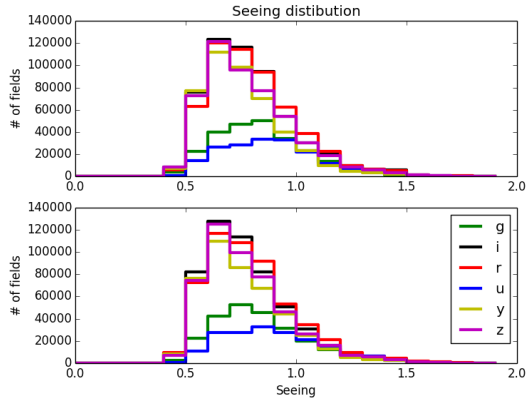


Figure 4. The 10 year seeing distribution of the LSST cadences in each filter. The baseline 2-detection cadence is given in the top panel, while the 4-detection cadence is shown in the lower panel.

3.1. Result for the Population of Objects Larger than 140m

The simulations show that with the 2-detection cadence, LSST reaches a completeness of 63% for the total NEO population larger than 140m after 10 years, and a 62% completeness for the PHA population larger than 140m (see Table 3.1). As expected, LSST is most efficient in finding objects among the Amor subpopulation, due to the fact that much of its time is spent observing the opposition regions of the sky where Amors are preferentially located. Conversely, LSST is less efficient at finding objects in the Aten and IEO subpopulations, since these tend to be distributed at lower solar elongations, and the two LSST cadences studied here spend relatively little time at solar elongations less than 90° (Fig. 1). High airmass image degradation and phase effects also play a significant role in the reduced detection of IEOs and Atens from ground based observatories. The completeness falls to 59% for the NEO population with diameters larger than 140m for the 4-detection cadence tested (see Table 3.1). The reduction in completeness is due to the fact that spending more exposures on each patch of sky necessitates a reduction in the amount of fresh sky covered each night. The effect of the 4-

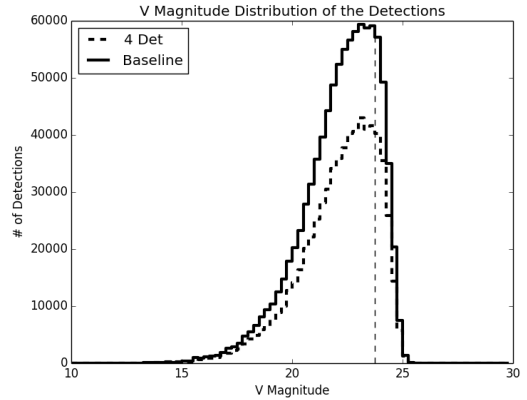


Figure 5. The V magnitude distribution of the individual detections in tracks for objects that were successfully found by the baseline and the 4-detection cadence surveys as seen in one of the 25 populations used in this paper. The vertical dashed line indicates a V magnitude of 23.75 mag.

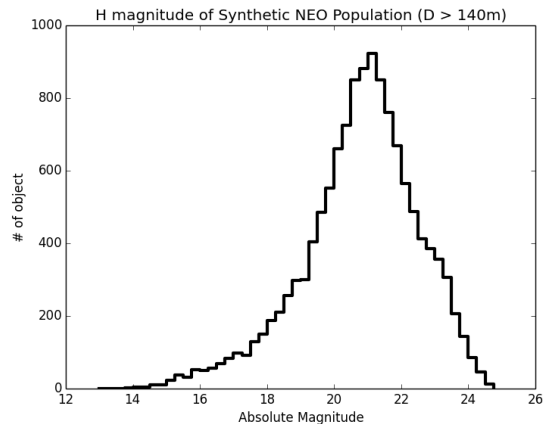


Figure 6. The absolute magnitude, H , of one of the synthetic NEO populations used in this paper. All the objects have diameters larger than 140m. About 23% of the objects have absolute magnitudes fainter than the $H = 22$ mag assumed as the default absolute magnitude of an 140m NEO.

detection cadence on the PHA completeness fraction is similar, dropping from 62% to 58%.

We have thus computed a more realistic value for the expected completeness of the LSST project in its

attempt to satisfy the 140m goal. We have used the project’s most recent simulated survey cadences, which contain the expected limiting magnitude for each field as affected by airmass, sky brightness, and weather. We point to several factors that resulted in a different estimate of the performance of LSST with regards to the NEO and PHA populations. First, we use an improved synthetic model for the NEO and PHA populations, where each object has size, albedo, and orbital elements based on the measured properties of the population from the NEOWISE survey (Mainzer et al. 2011a). This is a significant improvement over the synthetic population of 800 known PHAs used by Ivezić et al. (2014). Further, our analysis uses diameter to determine the completeness fraction, rather than the absolute magnitudes used in previous work. As pointed out above, a significant fraction of the PHAs with diameters larger than 140m have absolute magnitudes fainter than the 22 magnitude limit used in Ivezić et al. (2014). This is due to the fact that as determined by Mainzer et al. (2011c), $\sim 35\%$ of NEOs have low albedos. Also, Figure 5 shows the V magnitude of the detections of the objects found in the survey simulation for one of the populations used in combination with the baseline *enigma_1189* cadence. It shows that the peak of the distribution is in the $V \sim 23 - 23.75$ mag range, with the distribution turning sharply downwards at $V \sim 23.75$ mag. In both the baseline and the 4-detection cadence, only 18% of the observations of the detected synthetic objects have V magnitudes fainter than $V = 23.75$ mag. This limiting magnitude is shallower than the $V \sim 24 - 25$ assumed in Ivezić et al. (2007) and Ivezić et al. (2014).

These estimates of completeness assume that LSST would operate without any other surveys, past or future. However, the current NEOs surveys (CSS, Pan-STARRS, NEOWISE, etc.) have already discovered more than 13,000 NEOs, with an estimated current completeness for NEOs larger than 140m of $\sim 25\%$ (Mainzer et al. 2011a). Simulations of the current surveys estimate that the completeness will rise to $\sim 43\%$ at the start of the LSST survey, if the current surveys continue to operate unchanged. Our simulations show that the overlap of objects seen by the current surveys and LSST is significant, with the combination of the LSST and the current surveys at the end of the LSST operations reaching a completeness of 67% for NEOs larger than 140m (up from the 63% for LSST alone) in the 4-detection cadence case. For the PHAs, the completeness of LSST and the current surveys reaches 71% after the 10 year LSST survey is completed (up from the 58% for LSST alone). This significant overlap is due to the fact that both the current surveys and LSST operate by observing mainly at opposition. For the baseline 2-detection cadence, the combination of LSST and the current surveys

reaches 67% and 73% for the NEOs and PHAs larger than 140m, respectively.

Figure 7 shows the completeness of the PHA population larger than 140m for the 4-detection cadence. The 25 populations were run through all survey simulations and combined completeness values were derived by counting discovered objects as a function of time as the different surveys become available. Note that we choose to use the 4-detection cadence here, as this is what is used by current surveys and what is most often presented by other studies of survey performance, but using the LSST baseline 2-detection cadence only improves the completeness by a few percent. The performance of the current surveys is shown, along with the combination of the current surveys with the expected LSST. These are compared to the combined completeness of NEOCam and the current surveys, which reach 78% PHA completeness after five years (the NEOCam baseline mission) and 88% by 2031 (Mainzer et al. 2015). Operating both LSST and NEOCam offers the fastest means of reaching the 90% goal set by the George E. Brown, Jr. Near-Earth Object section of the NASA Authorization Act of 2005 (Public Law 109-155).

Table 1. LSST Yearly Completeness of NEOs > 140 m for 2-detection LSST Cadence

| Year | Total [%] | Interior [%] | Aten [%] | Apollo [%] | Amor [%] | PHAs [%] |
|------|------------|--------------|------------|------------|------------|------------|
| 1 | 12 \pm 1 | 1 \pm 1 | 9 \pm 1 | 12 \pm 1 | 14 \pm 1 | 13 \pm 1 |
| 2 | 28 \pm 1 | 2 \pm 1 | 18 \pm 1 | 27 \pm 1 | 32 \pm 1 | 29 \pm 1 |
| 3 | 38 \pm 1 | 2 \pm 1 | 24 \pm 1 | 36 \pm 1 | 44 \pm 1 | 38 \pm 1 |
| 4 | 45 \pm 1 | 2 \pm 1 | 30 \pm 1 | 43 \pm 1 | 52 \pm 1 | 44 \pm 1 |
| 5 | 49 \pm 1 | 2 \pm 1 | 35 \pm 2 | 48 \pm 1 | 56 \pm 1 | 48 \pm 1 |
| 6 | 53 \pm 1 | 2 \pm 1 | 38 \pm 2 | 52 \pm 1 | 61 \pm 1 | 52 \pm 1 |
| 7 | 56 \pm 1 | 2 \pm 1 | 40 \pm 2 | 55 \pm 1 | 64 \pm 1 | 55 \pm 1 |
| 8 | 59 \pm 1 | 2 \pm 1 | 43 \pm 2 | 58 \pm 1 | 67 \pm 1 | 58 \pm 1 |
| 9 | 61 \pm 1 | 2 \pm 1 | 45 \pm 2 | 59 \pm 1 | 69 \pm 1 | 60 \pm 1 |
| 10 | 63 \pm 1 | 2 \pm 1 | 47 \pm 2 | 61 \pm 1 | 70 \pm 1 | 62 \pm 1 |

Table 2. LSST Yearly Completeness of NEOs > 140 m for 4-detection LSST Cadence

| Year | Total [%] | Interior [%] | Aten [%] | Apollo [%] | Amor [%] | PHAs [%] |
|------|------------|--------------|------------|------------|------------|------------|
| 1 | 11 \pm 1 | 1 \pm 1 | 10 \pm 1 | 11 \pm 1 | 12 \pm 1 | 12 \pm 1 |

Table 2 continued

Table 2 (*continued*)

| Year | Total [%] | Interior [%] | Aten [%] | Apollo [%] | Amor [%] | PHAs [%] |
|------|-----------|--------------|----------|------------|----------|----------|
| 2 | 25 ± 1 | 1 ± 1 | 15 ± 1 | 24 ± 1 | 30 ± 1 | 26 ± 1 |
| 3 | 34 ± 1 | 1 ± 1 | 18 ± 1 | 33 ± 1 | 40 ± 1 | 34 ± 1 |
| 4 | 41 ± 1 | 1 ± 1 | 22 ± 1 | 40 ± 1 | 48 ± 1 | 41 ± 1 |
| 5 | 46 ± 1 | 1 ± 1 | 25 ± 2 | 45 ± 1 | 54 ± 1 | 46 ± 1 |
| 6 | 50 ± 1 | 1 ± 1 | 28 ± 2 | 49 ± 1 | 58 ± 1 | 49 ± 1 |
| 7 | 53 ± 1 | 1 ± 1 | 31 ± 2 | 52 ± 1 | 61 ± 1 | 52 ± 1 |
| 8 | 55 ± 1 | 1 ± 1 | 33 ± 2 | 55 ± 1 | 64 ± 1 | 55 ± 1 |
| 9 | 58 ± 1 | 1 ± 1 | 35 ± 2 | 57 ± 1 | 66 ± 1 | 57 ± 1 |
| 10 | 59 ± 1 | 1 ± 1 | 36 ± 2 | 58 ± 1 | 68 ± 1 | 58 ± 1 |

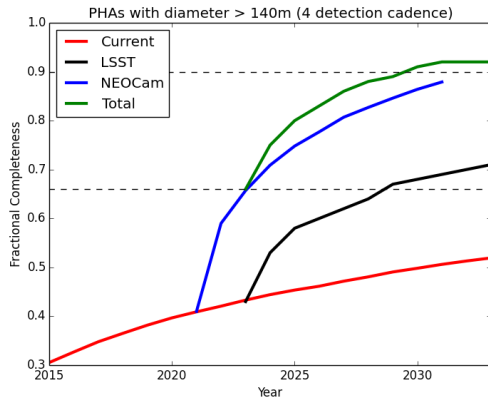


Figure 7. The completeness fraction as a function of time based on our simulations of the current surveys (red line), LSST plus the current surveys (black line), and the NEOCam survey plus the current surveys (blue line; [Mainzer et al. 2015](#)), along with the combined result from these three simulations (green line). Note that the NEOCam baseline mission is five years; the results of a ten year survey are also shown.

4. DISCUSSION AND CONCLUSION

We have performed a detailed survey simulation of the LSST performance using the current LSST baseline ca-

dence. The simulation shows that if the project is able to reliably generate tracklets using two detections per night and can link these tracklets into a track with a minimum of 3 tracklets covering more than a ~ 6 day length-of-arc, the survey would discover 62% of the PHAs larger than 140m in its projected 10 year survey lifetime. This completeness would be reduced to 58% if the 2-detection cadence cannot be implemented, and the more traditional 4-detection cadence is instead adopted. When including the estimated performance from the current operating surveys, assuming these would continue running until the start of LSST and perhaps beyond, the completeness fraction for PHAs larger than 140m would be 73% for the baseline cadence and 71% for the 4-detection cadence.

Our results differ from the estimates of [Ivezić et al. \(2007\)](#) and [Ivezic et al. \(2014\)](#), but are quite comparable to [Jones et al. \(2016\)](#) and [Chesley & Vereš \(2015, personal communication\)](#). Some reasons for the discrepancy include our choice of modeling the survey based on diameter, rather than the proxy population of objects with absolute magnitude $H < 22$ mag; choice of model input populations; and the difference among cadence choices. Our simulation accounts for the fact that a sizable fraction of NEOs larger than 140m are dark, with $H > 22$ mag ([Mainzer et al. 2011c, 2012b](#)). We have shown that using this proxy population is a less than optimal approach for estimating the ability of a survey to make progress towards the George E. Brown, Jr. goal of detecting and tracking 90% of the NEOs larger than 140m in diameter.

The advantages of operating both NEOCam and LSST are many. The combination of LSST and NEOCam creates observational redundancy (which improves reliability of individual tracklets) and the ability to extend orbital arcs, allowing potential impacts to be reliably predicted much farther into the future. The surveys observe complementary regions of orbital element phase space, with NEOCam observing more interior NEOs and Atens, and LSST preferentially detecting Amors near opposition. The combination of visible and IR fluxes will produce sizes, albedos, and color information, which gives insight into objects' probable composition (e.g. [Mainzer et al. 2012b](#)). Composition is a key uncertainty in understanding the potential damage that a given impactor could produce.

Even if LSST chooses to operate in the 2-detection cadence, which may lower its ability to link tracklets, linking its observations to objects found by NEOCam or other sources will provide an immensely powerful capability. Combining LSST observations with others will help to recover objects, secure orbits, and extend observational arcs.

5. ACKNOWLEDGEMENTS

This publication makes use of data products from NEOWISE, which is a project of the Jet Propulsion Laboratory/California Institute of Technology, funded by the National Aeronautics and Space Administration. This publication makes use of data products from the *Wide-field Infrared Survey Explorer*, which is a joint project

of the University of California, Los Angeles, and the Jet Propulsion Laboratory/California Institute of Technology, funded by the National Aeronautics and Space Administration. We gratefully acknowledge the support of the JPL High-Performance Computing Facility, which is supported by the JPL Office of the Chief Information Officer.

REFERENCES

- Alvarez, L. W., Alvarez, W., Asaro, F., & Michel, H. V. 1980, *Science*, 208, 1095
- Binzel, R. P., Lupishko, D., di Martino, M., Whiteley, R. J., & Hahn, G. J. 2002, *Asteroids III*, 255
- Bottke, W. F., Morbidelli, A., Jedicke, R., et al. 2002, *Icarus*, 156, 399
- Bowell, E., Hapke, B., Domingue, D., et al. 1989, in *Asteroids II*, ed. R. P. Binzel, T. Gehrels, & M. S. Matthews, 524–556
- Brown, P. G., Assink, J. D., Astiz, L., et al. 2013, *Nature*, 503, 238
- Chesley, S. R., & Vereš, P. 2015, in *AAS/Division for Planetary Sciences Meeting Abstracts*, Vol. 47, AAS/Division for Planetary Sciences Meeting Abstracts, 308.09
- Chyba, C. F., Thomas, P. J., & Zahnle, K. J. 1993, *Nature*, 361, 40
- Connolly, A. J., Angeli, G. Z., Chandrasekharan, S., et al. 2014, in *Society of Photo-Optical Instrumentation Engineers (SPIE) Conference Series*, Vol. 9150, Society of Photo-Optical Instrumentation Engineers (SPIE) Conference Series, 14
- Cutri, R. M., Wright, E. L., Conrow, T., et al. 2012, *Explanatory Supplement to the WISE All-Sky Data Release Products*, Tech. rep.
- Denneau, L., Jedicke, R., Grav, T., et al. 2013, *PASP*, 125, 357
- Diehl, T., & Dark Energy Survey Collaboration. 2012, *Physics Procedia*, 37, 1332
- Fukugita, M., Ichikawa, T., Gunn, J. E., et al. 1996, *AJ*, 111, 1748
- Goldstein, D. A., D’Andrea, C. B., Fischer, J. A., et al. 2015, *AJ*, 150, 82
- Grav, T., Jedicke, R., Denneau, L., et al. 2011, *PASP*, 123, 423
- Greenstreet, S., Ngo, H., & Gladman, B. 2012, *Icarus*, 217, 355
- Grieve, R. A. F. 1987, *Annual Review of Earth and Planetary Sciences*, 15, 245
- Hammel, H. B., Beebe, R. F., Ingersoll, A. P., et al. 1995, *Science*, 267, 1288
- Ivezić, Ž., Tabachnik, S., Rafikov, R., et al. 2001, *AJ*, 122, 2749
- Ivezić, Ž., Tyson, J. A., Jurić, M., et al. 2007, in *IAU Symposium*, Vol. 236, IAU Symposium, ed. G. B. Valsecchi, D. Vokrouhlický, & A. Milani, 353–362
- Ivezic, Z., Tyson, J. A., Abel, B., et al. 2014, *ArXiv e-prints*, arXiv:0805.2366
- Jones, R. L., Jurić, M., & Ivezić, Ž. 2016, in *IAU Symposium*, Vol. 318, IAU Symposium, ed. S. R. Chesley, A. Morbidelli, R. Jedicke, & D. Farnocchia, 282–292
- Jones, R. L., Yoachim, P., Chandrasekharan, S., et al. 2014, in *Society of Photo-Optical Instrumentation Engineers (SPIE) Conference Series*, Vol. 9149, Society of Photo-Optical Instrumentation Engineers (SPIE) Conference Series, 0
- Kohout, T., Gritsevich, M., Grokhovsky, V. I., et al. 2014, *Icarus*, 228, 78
- Larson, S. 2007, in *IAU Symposium*, Vol. 236, IAU Symposium, ed. G. B. Valsecchi, D. Vokrouhlický, & A. Milani, 323–328
- Levison, H. F., & Duncan, M. J. 1994, *Icarus*, 108, 18
- Lu, E. T., Reitsema, H., Troeltzsch, J., & Hubbard, S. 2013, *New Space*, 1, 42
- Mainzer, A., Grav, T., Bauer, J., et al. 2011a, *ApJ*, 743, 156
- Mainzer, A., Bauer, J., Grav, T., et al. 2011b, *ApJ*, 731, 53
- Mainzer, A., Grav, T., Masiero, J., et al. 2011c, *ApJ*, 736, 100
- . 2012a, *ApJ*, 752, 110
- Mainzer, A., Masiero, J., Grav, T., et al. 2012b, *ApJ*, 745, 7
- Mainzer, A., Grav, T., Bauer, J., et al. 2015, *AJ*, 149, 172
- McMurtry, C., Lee, D., Beletic, J., et al. 2013, *Optical Engineering*, 52, 091804
- Myhrvold, N. 2016, *PASP*, 128, 045004
- Ostro, S. J., & Giorgini, J. D. 2004, in *Mitigation of Hazardous Comets and Asteroids*, ed. M. J. S. Belton, T. H. Morgan, N. H. Samarasinha, & D. K. Yeomans, 38
- Shapiro, I. I., A’Hearn, M., Vilas, F., et al. 2010, *Defending Planet Earth: Near-Earth-Object Surveys and Hazard Mitigation Strategies* (National Research Council of The National Academies, Division of Engineering and Physical Sciences)
- Stokes, G. H., Yeomans, D. K., Bottke, W. F., et al. 2003, *Study to Determine the Feasibility of Extending the Search for Near-Earth Objects to Smaller Limiting Diameters*. Report of the Near-Earth Object Science Definition Team, Tech. rep.
- Wright, E. L., Eisenhardt, P. R. M., Mainzer, A. K., et al. 2010, *AJ*, 140, 1868
- Zahnle, K., & Mac Low, M.-M. 1994, *Icarus*, 108, 1